Title	Propagation Behavior of Root Crack in Y- and y-Grooved Restraint Cracking Test of 80kg/㎟ Class Steel on the Basis of AE Source Location Technique : Application of Acoustic Emission Technique for Weld Cracking (IV)(Materials, Metallurgy, Weldability)
Author(s)	Matsuda, Fukuhisa; Nakagawa, Hiroji; Morimoto, Yoshinori
Citation	Transactions of JWRI. 1979, 8(2), p. 241-247
Version Type	VoR
URL	https://doi.org/10.18910/9854
rights	
Note	

Propagation Behavior of Root Crack in Y- and y-Grooved Restraint Cracking Test of 80 kg/mm^2 Class Steel on the Basis of AE Source Location Technique†
– Application of Acoustic Emission Technique for Weld Cracking (IV) –

Fukuhisa MATSUDA*, Hiroji NAKAGAWA and Yoshinori MORIMOTO*****

Abstract

AE source location technique was applied to study the behavior of root cracking in restraint cracking test with Y- or y-groove with the aid of fractographic technique. Base metal used was weldable heat-treated high strength steel HT80 whose ultimate strength was 80kg/mm^2 class. Shielded metal-arc welding was done in the groove of the test specimen of HT80 and linear source location with AE technique was started after the completion of welding. Consequently two types of root cracks have been observed. The root crack in Type I mainly passes through the weld metal, and has a tendency to grow upwards namely toward the surface of weld metal. The root crack in Type II passes in the heat-affected zone in the early stage and then turned into the weld metal, and has a tendency to initiate and grow along the weld line in the early stage instead of their upward growth. The specimen which completely cracked in comparatively shorter period exhibits Type I.

KEY WORDS: (Acoustic Emission) (High Strength) (Cold Cracking) (Restraint) (Hydrogen Embrittlement)

1. Introduction

In the second report[1] of this title the authors discussed the behavior of root crack in 80kg/mm^2 class high strength steel HT80 with single bevel groove which passed through the heat-affected zone except for the final stage just before the complete cracking, and revealed that cracks occurred at several sites of the root edge in the early stage have a tendency to unite with one another by their propagation along the weld line instead of their upward propagation. Consequently AE events in AE source location were scattered along the whole weld line.

On the other hand, in the third report[2] the authors discussed the behavior of root crack in HY110 class steel with Y-groove which passed through the weld metal, and revealed that cracks occurred at the root edge in weld metal have a tendency to grow upwards namely toward the surface of weld metal. Consequently AE events generally concentrated in places where the cracks were growing upwards.

These behaviors of root crack and AE in these reports[1,2] are quite different each other. In these reports[1,2], however, there were discussed in extreme cases. Therefore it is interesting to know whether any in-between or mixed case can occur or not. Meanwhile, restraint cracking test with Y- or y-groove is often used in Japan, and it is usually said that the root crack generally has a tendency to enter into the weld metal in Y-grooved test and into heat-affected zone in y-grooved test. It is also said, however, that both cases are sometimes observed in HT80. So it is considered that the restraint cracking test with Y- or y-groove of HT80 is suitable to investigate in-between or mixed case of cracking path.

Therefore in this report AE source location technique has been applied to the restraint cracking test with Y- or y-groove of HT80, and the behaviors of root cracking have been discussed.

2. Materials Used and Experimental Procedures

A weldable heat-treated high strength steel HT80 whose ultimate strength was 80kg/mm^2 class was used for the restraint cracking test. The chemical composition is shown in **Table 1.** The configuration of test specimen is shown in **Fig. 1**, in which a Y- or y-groove was machined. The restraint welding in both sides of the groove was done with electron beam welding by each one pass from top

† Received on September 18, 1979
* Professor
** Research Instructor
*** Graduate Student (Presently, Komai Iron Works Co. LTD.)

Transactions of JWRI is published by Welding Research Institute of Osaka University, Suita, Osaka, Japan

Table 1 Chemical compositions of base metal and deposited metal

Material	Composition (wt.%)										
	C	Si	Mn	P	S	Cu	Ni	Cr	Mo	V	B
Base metal	0.13	0.27	0.86	0.011	0.004	0.25	1.08	0.50	0.43	0.04	0.0013
Deposited metal	0.06	0.63	1.36	0.010	0.005	–	1.73	0.24	0.44	–	–

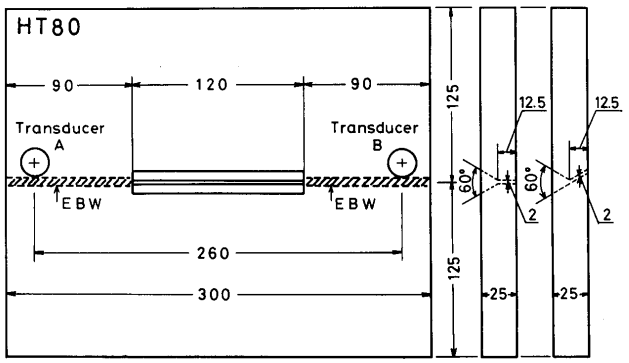

Fig. 1 Specimen configuration of restraint cracking test with Y- or y-groove

and back surfaces. The restraint intensity in the middle of groove length was about 1700kg/mm·mm according to the formula in case of uniformly distributed loads which was derived by Ueda, et al[3].

Shielded metal-arc welding was done with JIS D8016 (corresponding to AWS E11016) type electrode whose deposited metal had a ultimate strength of about 80kg/mm^2. The chemical composition of the deposited metal is also shown in Table 1. Baking condition of the electrode was varied in order to obtain various sizes of crack. The welding condition was 170A, 25V and 150mm/min. The details of welding procedure was just the same as that in the previous report[1].

Then, two AE transducers were set on the test specimen as shown in Fig. 1. AE measurement was started from 2min after the completion of welding and stopped after 48hr. The monitoring system, the procedure and the condition of AE measurement and the AE parameters measured were just the same as those in the previous report[1].

The procedures to measure the distribution of crack and crack ratios were also the same as those in the previous report[1].

3. Experimental Results and Discussions

3.1 Outline of types of cracks and AE

Table 2 summarizes the specimen number, the groove shape, the test condition, the results of the restraint crack-

Table 2 Summary of the results of restraint cracking test and AE measurements

Specimen number	Groove shape	Baking condition of electrode (°C x hr)	Preheating temperature (°C)	Cracked area (mm^2)	Crack ratio* (%)				Type of cracking path	AE data			
					C_a	C_s	C_f	C_r		Cumulative count**	Cumulative event count	S value	Max. ringdown counts/event
1	Y	400 x 0.8	room temp.	3	0.5	0	0	7	II	2000	23	2.80	600
2	Y	390 x 1	room temp.	4	0.7	1	0	11	II	6100	21	0.75	3300
3	Y	390 x 1	50	6	0.9	0	0	10	II	5400	39	2.40	1000
4	Y	400 x 1	room temp.	72	12	11	0	70	II	9000	34	1.13	2500
5	Y	390 x 1	room temp.	194	34	18	0	58	I	12400	34	0.60	5100
6	Y	390 x 1	room temp.	567	90	83	76	98	II	376900	192	0.42	>10000
7	Y	as received	room temp.	585	100	100	100	100	I	459000	251	0.36	>10000
8	Y	200 x 1	room temp.	636	100	100	100	100	I	641800	350	0.36	>10000
9	y	390 x 1	room temp.	1	0.2	0	0	4	II	4000	19	0.89	2700
10	y	410 x 1	room temp.	20	4	0	0	17	II	6300	32	1.24	2200
11	y	410 x 0.7	room temp.	242	42	40	26	54	I	36500	64	0.71	4900
12	y	410 x 1	room temp.	329	59	58	45	70	I	154800	100	0.39	9700
13	y	400 x 1	room temp.	383	61	55	15	88	II	59700	87	0.57	7100
14	y	400 x 0.8	room temp.	586	100	100	100	100	I	278200	191	0.44	9900
15	y	200 x 1	room temp.	591	100	100	100	100	I	664400	387	0.35	>10000
16	y	390 x 1	room temp.	613	100	100	100	100	II	229900	184	0.59	7400

*C_a is crack ratio on fractured surface, C_s is cross sectional crack ratio, C_f is surface crack ratio and C_r is root crack ratio.

**AE cumulative count is the mean value of two channels.

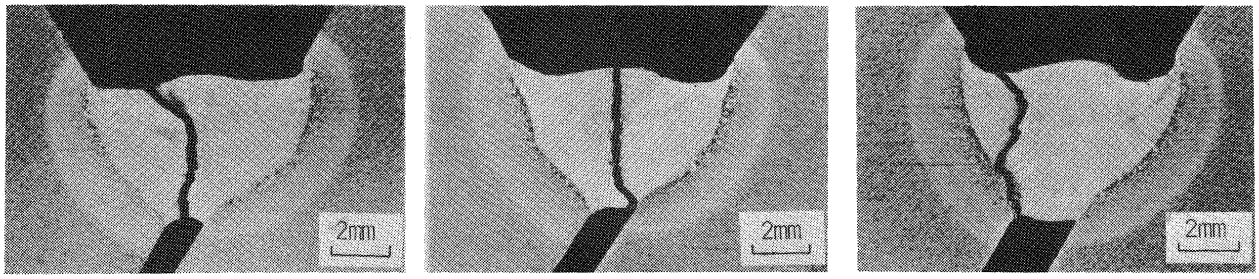

(a) typical example of Type I (b) sporadic example of Type I (c) typical example of Type II

Fig. 2 Macrostructure of transverse cross section of welded zone

ing test and AE data, where cracked area and crack ratios are defined in the previous report[1]. Namely, the cracked area is area in mm^2 measured on artificially fractured surface, C_a is crack ratio on the artificially fractured surface, C_s is cross sectional crack ratio, C_f is surface crack ratio and C_r is root crack ratio. The column giving "Type of cracking path" in Table 2 means the following. In Type I the root crack predominantly passed through the weld metal whose typical example is shown in **Fig. 2(a)**, although in some cases the root crack sporadically and slightly entered into the heat-affected zone as seen in **Fig. 2(b)**. In Type II the root crack in the early stage always passed in the heat-affected zone to a certain extent and then turned into the weld metal whose typical example is shown in **Fig. 2(c)**, although the root crack in the case of small crack ratio occurred in only the heat-affected zone. As seen in Table 2, these types didn't depend on the groove shape. Generally insufficient baking condition of electrode had a tendency to result in Type I, and thus the specimen in Type I completely cracked in comparatively shorter period than that in Type Type II.

In connection with these types, AE parameters also closely depended on the type of crack path.

3.2 AE characteristics and behavior of root crack in Type I

Figure 3 shows the changes in AE cumulative count and AE cumulative event count vs. time in specimen No. 11 whcih is a typical example of Type I, and **Fig. 4** shows the change in AE source location in the same specimen during the time intervals shown in Fig. 4. Relative location in the abscissain Fig. 4 is defined to be 0% at the left transducer and 100% at the right one in Fig. 1, and the increase in the relative location agrees with the welding direction. The AE emitted in the welds lie between about 20 and 80% of relative location, the range of which is indicated by arrows in Fig. 4. Both AE cumulative count and event count in Fig. 3 increased gradually and intermittently from the start of measurement till about 13hr, and then they almost stopped. At about 6hr in the middle, a part of the crack was visible with the naked eyes on the surface of weld metal near the crater.

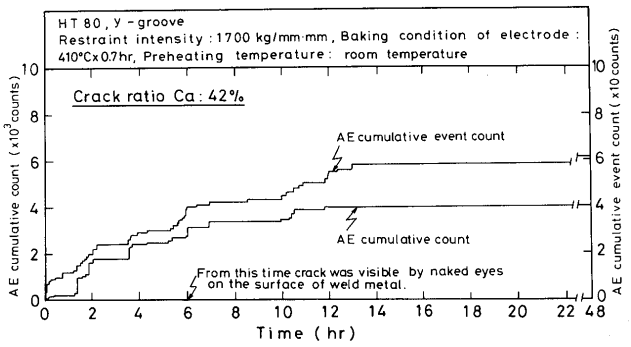

Fig. 3 Changes in AE cumulative count and cumulative event count vs. time in specimen No. 11 which belongs to Type I

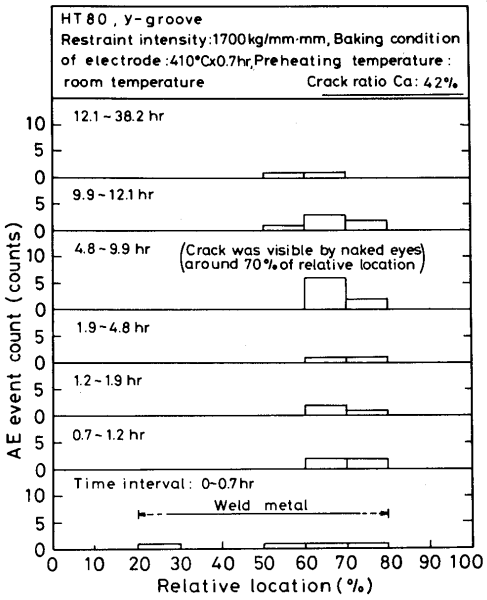

Fig. 4 Change in AE source location vs. time in the same specimen as that in Fig. 3

AE events in Fig. 4 were sporadic during the time intervals 0 to 0.7hr, and then concentrated in 60 to 80% of relative location thereafter. During the time interval 9.9 to 38.2hr AE events also concentrated in 50 to 60% of relative location. Its final AE source location is shown in **Fig. 5**. According to this result in Fig. 4, the propagation behavior of this root crack is as follows: A few cracks in the first stage occurred at the root edge near the crater and then propagated toward the surface of weld metal. Then a part of them reached the surface of weld metal. Subsequently another crack adjoining the first cracks propagated toward the surface of weld metal. The crack, however, stopped owing to escape of diffusible hydrogen.

The macrofractograph of this specimen and its sketch, which is written with a magnification of about two times in the height direction, are shown in **Fig. 6**. The total of

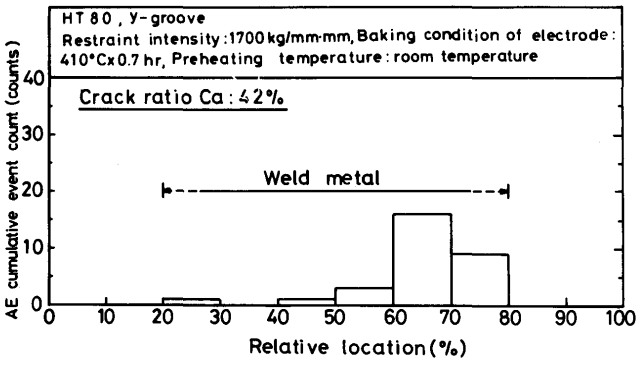

Fig. 5 Final AE source location in the same specimen as that in Figs. 3 and 4

IG_C, QC and D_S are the cracked region and A_F is artificially fractured region after the cracking test. The IG_C region microscopically gives a feature shown in **Fig. 7(a)** which is mainly composed of intergranular fracture along columnar crystal boundary of prior austenite and partly of quasi-cleavage affected by hydrogen. Thus the IG_C region cracked in the weld metal. The QC region macroscopically gives a non-directional appearance, and microscopically gives a feature shown in **Fig. 7(b)** which is mainly composed of quasi-cleavage affected by hydrogen. The QC region cracked in the heat-affected zone. The D_S region corresponds to the shear lip zone and microscopically gives shear dimple fracture.

Comparing Fig. 5 with Fig. 6, the AE source location in Fig. 5 well agrees with the distribution of crack in Fig. 6. Therefore, when the root crack mainly pass through the weld metal, the crack has a tendency to grow toward the surface of weld metal instead of growing parallel to the weld line. Consequently AE events also have a

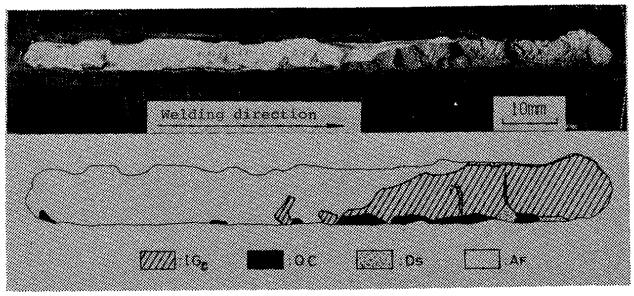

Fig. 6 Oxidized and fractured surface and its sketch of the same specimen as that in Figs. 3 to 5

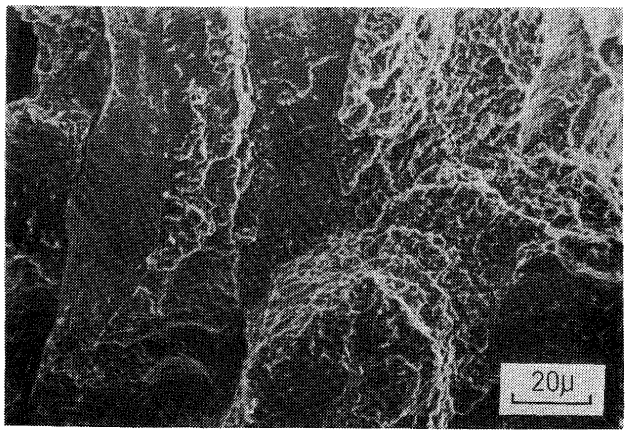

(a) mainly intergranular and partly hydrogen-induced quasi-cleavage fractures in weld metal (defined as IG_C region)

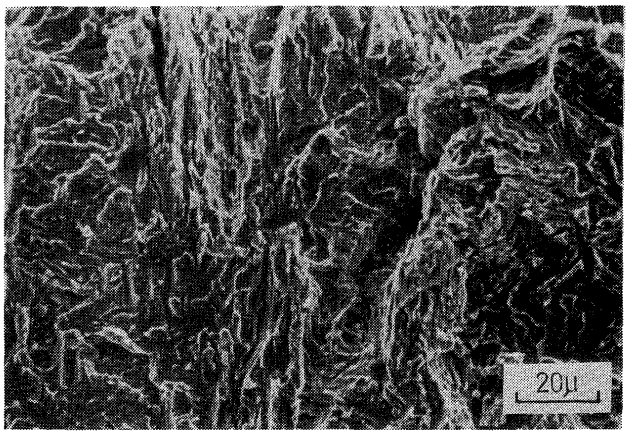

(b) mainly hydrogen-induced quasi-cleavage fracture in heat-affected zone (defined as QC region)

Fig. 7 Typical microfactographs of root crack with scanning electron microscope

tendency to concentrate in tha places where the cracks are propagating toward the surface of weld metal.

These behaviors of root crack and AE are similar to those in HY110 class steel with Y-groove[2]. The root crack in Type I of HT80, however, was somewhat easier to enter into the heat-affected zone than HY110 class steel. Consequently the concentration of AE events in AE source location was occasionally obscure.

3.3 AE characteristics and behavior of root crack in Type II

Figure 8* shows the changes in AE cumulative count and AE cumulative event count vs. time in specimen No. 16 which is a typical example of Type II, and **Fig. 9** shows the change in AE source location in the same specimen during the time intervals shown in Fig. 9. In Fig. 8 occurrence of AE is little till about 2.5 hr except for the incipient increase, and then both AE cumulative count and event count increased gradually and intermittently till about 7.9hr. Then the occurrence of AE ceased from 7.9 to 9.7hr. The existence of this temporary cessation of AE is an obvious feature of Type II. During the time intervals 0 to 7.9hr in Fig. 9, the AE events were emitted intermittently from place to place over the whole weld line. This behavior in AE source location is similar to that in HT80 with single bevel groove in the second report[1]. This suggests that the root crack extended over the heat-affected zone near the root edge along the whole weld line by 7.9hr.

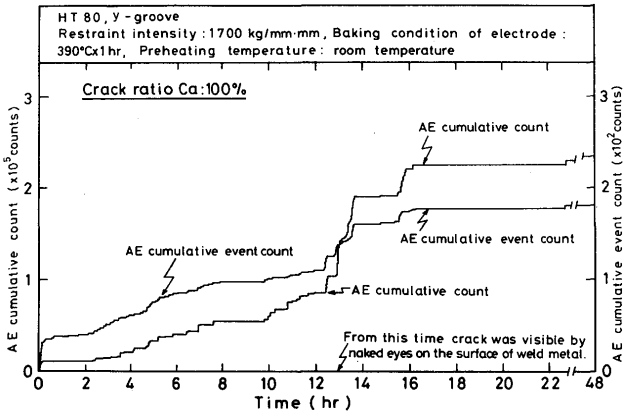

Fig. 8 Changes in AE cumulative count and cumulative event count vs. time in specimen No. 16 which belongs to Type II

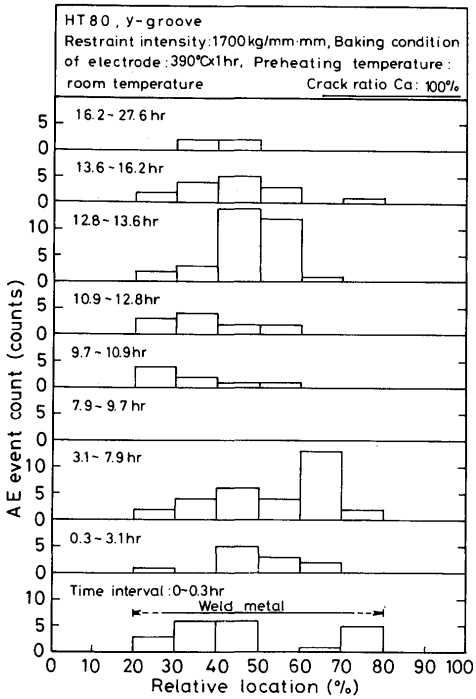

Fig. 9 Change in AE source location vs. time in the same specimen as that in Fig. 8

After the cessation during 7.9 to 9.7hr, both AE cumulative count and event count again increased gradually and intermittently till about 16.2hr. Especially the increasing rate of AE is large between 12.8 to 13.6hr, when crack was visible with the naked eyes on the surface of weld metal. The specimen almost completely cracked at about 16.2hr. The AE events after 9.7hr in Fig. 9 also scattered from place to place over the weld line.

Its final AE source location is shown **in Fig. 10.** There are much AE events in 40 to 50% of relative location, where AE were actively emitted during 12.8 to 13.6 hr in Fig. 8.

The macrofractograph of this specimen and its sketch are shown in **Fig. 11.** The QC in the heat-affected zone extends over the whole weld line near the root edge, which is similar to the crack distribution in HT80 with single bevel groove[1]. Then, there are IG_C region in the upper part of QC region, which was not generally formed in HT80 with single bevel groove. This difference arises as

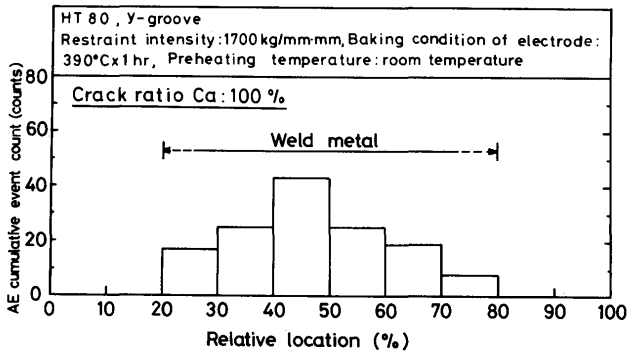

Fig. 10 Final AE source location in the same specimen as that in Figs. 8 and 9

*Pay attention to difference in scale of the ordinate among Figs. 3, 8, 12 and 14.

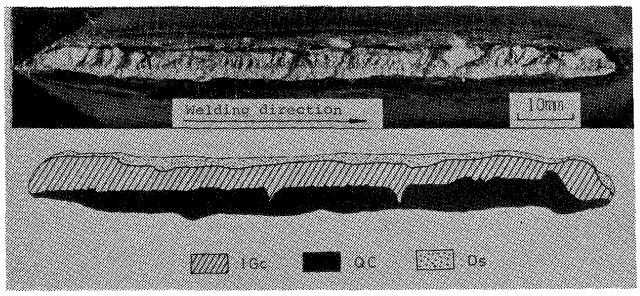

Fig. 11 Light fractograph and its sketch of the same specimen as that in Figs. 8 to 10

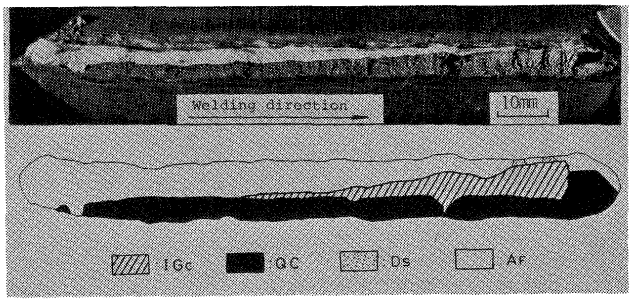

Fig. 13 Oxidized and fractured surface and its sketch of the same specimen as that in Fig. 12

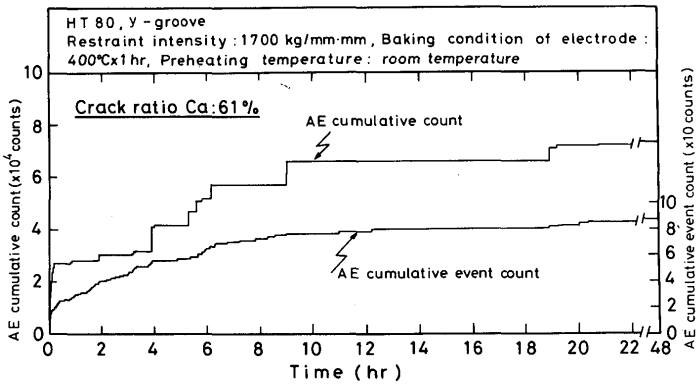

Fig. 12 Changes in AE cumulative count and cumulative event count vs. time in specimen No. 13. which belongs to Type II.

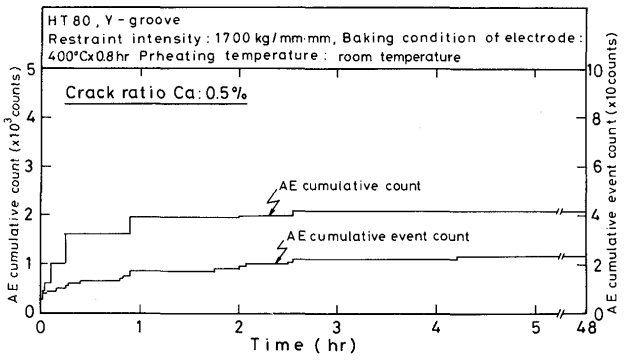

Fig. 14 Changes in AE cumulative count and cumulative event count vs. time in specimen No. 1 which belongs to Type II and has very small cracks.

an inevitable consequence from the difference in the groove shape.

As mentioned in Fig. 8, one of the characteristics of Type II is the existence of temporary cessation of AE. It is expected that this corresponds to an incubation period when the root crack in the heat-affected zone turns into the weld metal, because it is considered that still more enrichment of diffusible hydrogen to the crack tip is required for the crack growth into the weld metal due to the lower hardness in the weld metal than in the heat-affected zone. In the following, the results which are considered to confirm this are explained. **Figure 12** shows the changes in AE cumulative count and AE cumulative event count vs. time in specimen No. 13 belonging to Type II which has 61% of crack ratio Ca. In Fig. 12 the temporary cessation continued from about 12 to 19hr, then AE were again emitted from about 19 to 21hr and then almost stopped. The macrofractograph of this specimen and its sketch is shown in **Fig. 13**, where QC in the heat-affected zone extends almost over the whole weld line and small IG_C region is formed in the upper part of QC. Thus it is considered that the temporary cessation of AE is related to the incubation period when the root crack in the heat-affected zone turns into the weld metal.

By the way, AE events after the temporary cessation, namely after 9.7hr in Fig. 9 did not concentrate to any relative location, but rather were scattered in spite of the crack propagation in the weld metal. As regards this, the distribution of diffusible hydrogen is considered to be one of the major factor, but the detailed reason is incomprehensible now.

Then, **Fig. 14** shows the changes in AE cumulative count and AE cumulative event count vs. time in specimen No. 1 belonging to Type II where very small root crack occurred. Both AE cumulative count and event count increased gradually and intermittently after the start of measurement, and then stopped at about 4.2hr. In any specimen where crack ratio is little AE stopped by about 5hr. In AE source location AE events were scattered along the weld line, and several tiny root cracks were sporadically distributed in the heat-affected zone at the root edge along the weld line on the macrofractograph.

Other differences between Types I and II are as follows: The time after which the crack was visible on the surface of weld metal is earlier in Type I than in Type II, which is obvious in comparison between Figs. 3 and 8.

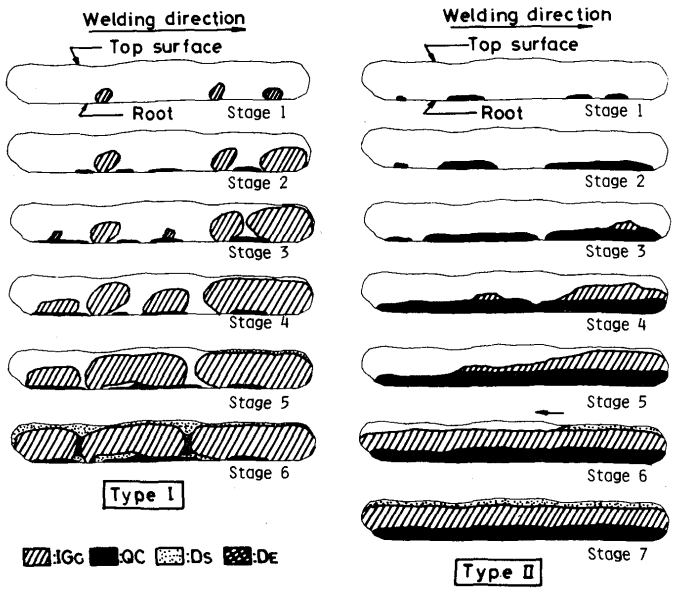

Fig. 15 Estimated propagation behavior of root crack

This time in every specimen in Type I was within about 6hr. Moreover in comparison between specimens partially cracked, AE in Type I stopped in shorter period than in Type II.

3.4 Illustration of propagation behavior of root crack

Summarizing the results above mentioned and other data together, the propagation behavior of root crack is illustrated in **Fig. 15**.

The crack path of Type I is similar to that in HY110 class steel and as follows. The root cracks occur in the weld metal at a few sites of root edge (Stage 1). They propagate toward the surface of weld metal, and at the same time tiny root cracks occur in the heat-affected zone (Stage 2). Then they propagate further and root cracks in the heat-affected zone easily turn into the weld metal (Stage 3 to 4). Subsequently a part of them reaches the surface of weld metal in shear lip mode (Stage 5). Finally, when the stress condition which has imposed on uncracked portion becomes a critical condition, this portion fractures rapidly in dimple pattern (Stage 6).

The crack path of Type II is partly similar to that in HT80 with single bevel groove and as follows. The root cracks occur in the heat-affected zone at several sites of root edge (Stage 1), and propagates along weld line in order to link each other (Stage 2). When they unite almost completely, a part of them turns into the weld metal after an incubation period (Stage 3), and this turn occurs at other places (Stage 4 to 5). Then a part of crack reaches the surface of weld metal in shear lip mode (Stage 6) and shear lip extends over the whole weld line (Stage 7).

If the diffusible hydrogen content is relatively low, the root cracking ends by Stage 5 in Type I or Stage 6 in Type II. If the diffusible hydrogen content is extremely low, the root cracking occurs only in State 1 in Type II.

4. Conclusion

AE source location technique was utilized for studying the propagation behavior of root crack in the restraint cracking test with Y- or y-groove of HT80. Main conclusions obtained are as follows:

(1) The root cracks are classified into two types, namely Types I and II, independent of Y- and y-groove. The root crack in Type I mainly passes through the weld metal, and that in Type II passes in the heat-affected zone in the early stage and then turns into the weld metal.

(2) Generally insufficient condition of electrode had a tendency to result in Type I, and thus the specimen in Type I completely cracked in comparatively shorter period than that in Type II.

(3) The root crack in Type I occurred at a few sites of root edge has a tendency to grow upwards, namely toward the surface of weld metal. Consequently AE events in AE source location concentrate in the place where the crack are growing upwards.

(4) The root cracks in Type II occurred at several sites of root edge in the early stage have a tendency to unite easily with one another by their propagation along the weld line instead of their upward growth. Consequently AE events are scattered along the whole weld line. Another obvious feature of AE in Type II is the existence of a certain temporary cessation of AE, which is considered to be related to an incubation period when the root crack in the heat-affected zone turns into the weld metal.

(5) Other differences between Types I and II are as follows: (a) The time after which the crack is visible on the surface of weld metal is earlier in Type I than in Type II. (b) In comparison between specimens partially cracked, AE stopped in shorter period in Type I than in Type II.

References

1) F. Matsuda, et al: Trans. JWRI, Vol. 7 (1978), No. 2, p. 203.
2) F. Matsuda, et al: Trans. JWRI, Vol. 8 (1979), No. 1, p. 97.
3) Y. Ueda, et al: Trans. JWRI, Vol. 7 (1978), No. 1, p. 11.